

University of Groningen

## Bonding along metal-oxide interfaces

Haarsma, Hendrik

**IMPORTANT NOTE:** You are advised to consult the publisher's version (publisher's PDF) if you wish to cite from it. Please check the document version below.

*Document Version*

Publisher's PDF, also known as Version of record

*Publication date:*

2003

[Link to publication in University of Groningen/UMCG research database](#)

*Citation for published version (APA):*

Haarsma, H. (2003). *Bonding along metal-oxide interfaces*. s.n.

### Copyright

Other than for strictly personal use, it is not permitted to download or to forward/distribute the text or part of it without the consent of the author(s) and/or copyright holder(s), unless the work is under an open content license (like Creative Commons).

The publication may also be distributed here under the terms of Article 25fa of the Dutch Copyright Act, indicated by the "Taverne" license. More information can be found on the University of Groningen website: <https://www.rug.nl/library/open-access/self-archiving-pure/taverne-amendment>.

### Take-down policy

If you believe that this document breaches copyright please contact us providing details, and we will remove access to the work immediately and investigate your claim.

Downloaded from the University of Groningen/UMCG research database (Pure): <http://www.rug.nl/research/portal>. For technical reasons the number of authors shown on this cover page is limited to 10 maximum.

# CHAPTER 2

## Theory

*A large set of physical models is available to calculate structural features of metal/ceramic interfaces. In this chapter, we will explore current models and discuss the strong and the weak points. We will draw conclusions as to which model is suitable for our own computational approach. A model is designed in such a way that the interactions are derived from a physical description being tractable from a computational viewpoint. In particular, the model has to provide a framework to investigate the atomic structure, including relaxations, near complex metal/ceramic interfaces, which are too large to tackle with first-principle calculations. The accuracy of the model will be demonstrated in the subsequent chapters in which the results for various interface systems are presented and discussed.*

### 2.1 Introduction

As explained in Chapter 1 metal-ceramic interfaces play an important role in modern materials technology. In fact, important processes that are controlled by interface phenomena, such as decohesion and segregation, occur in a very narrow region, of the order of a few lattice spacings, where the two materials join. To gain a more fundamental understanding of the properties of metal-ceramic interfaces we are in particular interested in performing structural optimizations on an atomic scale. This chapter is devoted to a critical evaluation of existing models, from which conclusions will be drawn for our own approach. Our objective is to design a computational framework, that on one hand is based a sound physical description provided by quantum

mechanics but on the other hand is still tractable for very complex systems like metal-ceramic interfaces. It should be emphasized that these heterophase interfaces are like discontinuities for both electrons and atoms. Then, the central question is how to deal with these shape transitions because nature always tries to avoid discontinuities.

## 2.2 Different approaches

The interactions between atoms are dominated largely by the interactions that take place between the electron clouds of the atoms. To model the interactions between atoms correctly it is therefore necessary to give a correct description of the behavior of the electrons and this is usually done with the help of the time-independent Schrödinger equation. The time independent Schrödinger equation for a system with N-particles reads<sup>1</sup>:

$$\left[ -\hbar^2 \left( \frac{1}{2m_1} \frac{\delta^2}{\delta \vec{r}_1} + \dots + \frac{1}{2m_N} \frac{\delta^2}{\delta \vec{r}_N} \right) + V_{eff}(\vec{r}_1, \dots, \vec{r}_N) \right] \Psi(\vec{r}_1, \dots, \vec{r}_N) = E \Psi(\vec{r}_1, \dots, \vec{r}_N) \quad (2.1)$$

In the Schrödinger equation the wavefunction of all the particles is given by  $\Psi(\vec{r}_1, \dots, \vec{r}_N)$ , where  $\vec{r}_i$  represent the position vector of particle  $i$ . The probability of finding the particles in a certain position (particle 1 in position  $\vec{r}_1$ , particle 2 in position  $\vec{r}_2$  and so on) is given by the following equation:

$$P(\vec{r}_1, \dots, \vec{r}_N) = |\Psi(\vec{r}_1, \dots, \vec{r}_N)|^2 d\vec{r}_1 \dots d\vec{r}_N \quad (2.2)$$

Where  $\Psi(\vec{r}_1, \dots, \vec{r}_N)$  is normalized:

$$\int_{-\infty}^{\infty} P(\vec{r}_1, \dots, \vec{r}_N) d\vec{r}_1 \dots d\vec{r}_N = 1 \quad (2.3)$$

In the Schrödinger equation, the term  $V_{eff}(\vec{r}_1, \dots, \vec{r}_N)$  represents the effective potential. As we will see later this can be the potential from nuclei and from other electrons. The wavefunction has a certain eigenvalue  $E$  that represents the energy in the external potential.

To solve this equation for even a very simplified model of a heterophase interface is quite cumbersome, if not impossible. In general, at a heterophase interface two different materials are present, one on either side. These materials in general will have different lattice parameters. It requires a large

computational cell or a change in periodicity of one of the systems to match the periodicity of the other system. Even with the latter option, the computational cells for interfaces remain rather large, because the dimension perpendicular to the interface should be large enough allowing the atoms farther away from the interface in a situation comparable to the bulk.

To be able to perform calculations of an interface system it is necessary to simplify the model as much as possible without losing physical relevance. Several simplifications have been introduced in order to make the calculations on larger systems tractable.

The first simplification that is made is to assume that the nuclei move so slow with respect to the movement of the electrons that it can be assumed that the nuclei are standing still. This simplification is called the Born-Oppenheimer approximation<sup>2</sup>. This simplifies the model because the locations of the nuclei are now input parameters and are not longer free variables. Despite this simplification, the model is not simple enough to be able to perform calculations with it; all the electrons still affect each other.

The influence of the nuclei is now described by an additional term of the effective potential. This term is given by the following equation with  $N$  referring only to electrons:

$$V_{Nuclei}(\vec{r}_1, \dots, \vec{r}_N) = \frac{1}{4\pi\epsilon} \sum_{i=1}^N \sum_{j=1}^{N_{nuclei}} \frac{Z_j}{|\vec{r}_i - \vec{R}_j|} \quad (2.4)$$

Hohenberg and Kohn proved a fundamental theorem<sup>3</sup>, namely instead of using the many electron wavefunction it is possible to use the electronic charge density for the interactions. The simplification comes from the fact that the electronic charge density depends only on the coordinates in the point of interest and not on the locations of all electrons, as the many electron wavefunction does. A complication is however that the electronic charge density depends on the many electron wavefunction.

The next important simplification brought forward by Kohn and Sham<sup>4</sup> is that the electronic ground state can be described by  $N$  single electron equations instead of a single many-electron equation. The influences of all the other electrons are now described in the effective potential that the electron experiences.

This simplifies the Schrödinger equation to the following equation, i.e. the wavefunction for electron  $i$ . In the effective potential  $V_{eff}(\vec{r}_i)$  the influence of all the other electrons has to be taken into account. The energy of the wavefunction of electron  $i$  is given by the eigenvalue of the wavefunction,  $\epsilon_i$ .

$$-\frac{\hbar^2}{2m_i} \frac{\delta^2}{\delta \vec{r}_i^2} \psi_i(\vec{r}_i) + V_{eff}(\vec{r}_i) \psi_i(\vec{r}_i) = \epsilon_i \psi_i(\vec{r}_i) \quad (2.5)$$

For the Hartree potential<sup>2</sup> almost the same approach is made. In this approach, all the electrons move in an external potential caused by the electron density and the nuclei. The part of the effective potential, due to the electrons, is written as:

$$V_H(\vec{r}) = \int \frac{1}{4\pi\epsilon} \frac{\rho(\vec{r}')}{|\vec{r} - \vec{r}'|} d\vec{r}' \quad (2.6)$$

In this equation  $\rho(\vec{r})$  is the electron density in  $\vec{r}$ . The relation between the wavefunctions of the electrons and the electron density is given by:

$$\rho(\vec{r}) = \sum_i n_i |\psi_i(\vec{r})|^2 \quad (2.7)$$

Because of the electron density, this potential includes the unphysical self-interaction of the electrons.

To get a physically more correct description the exchange-correlation term should be included in the effective potential. The exchange-correlation term exists of two components: the exchange and the correlation energy. These terms are related to the Coulomb repulsion that the electrons have and the repulsion between electrons due to the exclusion principle for electrons with the same spin, respectively.

In addition to the Hartree equations the exchange correlation potential is included in the effective potential of the Kohn-Sham equations<sup>4</sup>. The effective potential consists of three components: the potential due to the nuclei, the potential due to electron density and the exchange-correlation term:

$$V_{eff}(\vec{r}) = V_{Nuclei}(\vec{r}) + V_H(\vec{r}) + V_{xc}(\vec{r}) \quad (2.8)$$

The Kohn-Sham equations are exact, but solving them is problematic because the exact forms of the exchange-correlation potential and energy are not known. The approximation that is commonly used is to solve this is in the so-called Local Density Approximation (LDA) in which the exchange-correlation energy

only depends on the local value of the charge density. No variations in the charge density are taken into account. In the Local Density Approximation the potential of the exchange-correlation is given by:

$$V_{xc}(\vec{r}) = \frac{\delta E_{xc}[\rho(\vec{r})]}{\delta \rho(\vec{r})} \quad \text{where: } E_{xc}[\rho(\vec{r})] = \int \varepsilon_{xc}(\rho(\vec{r}))\rho(\vec{r})d\vec{r} \quad (2.9)$$

In this equation  $\varepsilon_{xc}(\rho(\vec{r}))$  represents the exchange-correlation energy per electron of a uniform electron gas with density  $\rho(\vec{r})$ , and  $E_{xc}[\rho(\vec{r})]$  is the exchange-correlation energy of the given electron density.

For the Kohn-Sham equations, it is necessary to calculate the charge density self-consistently. This means that from the initial charge density that is used as input, a new charge density is calculated. This is repeated until the in- and output charge densities are identical. For each step, the energy of the system can be approximated by the following equation:

$$\begin{aligned} E^{HKS}[\rho^{out}] = & \sum_i n_i^{out} \varepsilon_i^{out} - \int \frac{1}{4\pi\epsilon} \frac{\rho^{out}(\vec{r})\rho^{in}(\vec{r}')}{|\vec{r} - \vec{r}'|} d\vec{r}d\vec{r}' + \\ & \frac{1}{2} \int \frac{1}{4\pi\epsilon} \frac{\rho^{out}(\vec{r})\rho^{out}(\vec{r}')}{|\vec{r} - \vec{r}'|} d\vec{r}d\vec{r}' - \int \rho^{out}(\vec{r})V_{xc}(\rho^{in}(\vec{r}))d\vec{r} + E_{xc}[\rho^{out}(\vec{r})] + E_{NN} \end{aligned} \quad (2.10)$$

The first term on the right ( $\sum_i n_i^{out} \varepsilon_i^{out}$ ) is the sum of each eigenvalue of the wavefunction of all electrons. The second and the third term give the energy due to the Coulomb interactions of the electrons. These two terms are followed by two terms that describe the energy of the exchange-correlations interactions and the last part is the energy of the Coulomb interactions of the nuclei.

The energy that is calculated with this method is always larger than the ground state energy, unless the input charge density equals the output charge density in which case the ground state is found. To get a reasonable estimate of the total energy, without solving the Kohn-Sham equations, the following equation is found by Harris<sup>5</sup> and by Foulkes<sup>6</sup>.

$$\begin{aligned} E^{HF}[\rho^{in}, \rho^{out}] = & \sum_i n_i^{out} \varepsilon_i^{out} - \int \frac{1}{4\pi\epsilon} \frac{\rho^{in}(\vec{r})\rho^{in}(\vec{r}')}{|\vec{r} - \vec{r}'|} d\vec{r}d\vec{r}' - \\ & \int \rho^{in}(\vec{r})V_{xc}(\rho^{in}(\vec{r}))d\vec{r} + E_{xc}[\rho^{in}(\vec{r})] + E_{NN} \end{aligned} \quad (2.11)$$

The strength of this formulation lies in a couple of points. The first strong point is that the calculated energy is the same as the calculated energy with Eq. (2.10), provided the electrons are in the ground state. Another point is that for the

determination of the exchange-correlation energy, it is possible to use the input charge density, instead of the output density and therefore it is possible to use the charge densities of the single atoms as input densities. With an appropriate choice of the input density, it is possible to end up with integrals that can be evaluated with relative ease.

In these calculations the distribution of all the electrons are calculated, including the electrons that are in the cores of the atom. These core electrons are shielded from the electron of other atoms by the electrons in the outer shells of the atom, and therefore they do not or hardly contribute to the bonding that takes place between two atoms. This justifies the use of pseudo-potentials, in which the core electrons are replaced by rather simple pseudo-potentials to describe their behavior.

Upon further simplification of the description of the interactions between the atoms, one arrives at the area of the tight binding theory<sup>7</sup>. To simplify the description of the interactions, some of the integrals that have to be solved in quantum mechanical calculations are neglected or simplified, by fitting to experimental data. Because of the usage of parameters that have to be fitted, one has to ensure that the values of the parameters are valid for the problem under investigation.

In the second moment approximation to the tight binding scheme, use is made of the information of the second moment of the local density of states and higher moments are not included. In the approximation, the covalent bonds energies are calculated as the square root of a sum of pair potentials. There is also a repulsive term, which is constructed also from pair potentials. All the pair potentials that are used in this approximation are fitted to experimental data. The following formula is used for the determination of the energy of the system.

$$E_{tot} = \frac{1}{2} \sum_i \sum_{j \neq i} V(\vec{r}_{ij}) - \sum_i \sqrt{\sum_{j \neq i} \phi(\vec{r}_{ij})} \quad (2.12)$$

Actually, this is a special case of the Embedded Atom Method<sup>8</sup>, in which the square root is not a priori assumed. Further, it is the same in the sense that also pair potentials are used, which is to be fitted to experimental data. The embedded atom method is based on the effective medium theory, in which the model is simplified in such a way that the picture boils down to the submerging of the atom in the free electron gas of the other atoms. Depending on the model

that is used this free electron gas is either uniform in space or calculated self-consistently.

An even simpler model would be to use only pair-wise interactions without making use of the square root as displayed in the previous equation. This simplification does in general not bring a very big difference in computational effort. In some cases the quality of the description of the interactions decreases strongly, i.e. an incorrect response to the coordination number occurs and the elastic constants attain wrong values. For most metals it can be said that upon increasing the coordination number results in a decreasing strength of the individual bonds. With only pair potentials, this effect cannot be properly described but in the second moment approximation, it is an automatic outcome. In the second moment approximation, the calculated values of some of the elastic constants will prove to be physically correct, while for the pair potentials this is not the case.

### 2.3 The description used in this thesis

#### *Interactions between the metal atoms*

For the description of the interactions among the metal atoms, the second moment approximation in the tight binding scheme is chosen. This model is adopted because of the results that can be achieved with relatively little computational effort. The computational simplicity of the model allows the use of large computational cells containing many atoms, which allows calculations of more complex systems than is possible with first-principle calculations. The down side of this scheme is that the descriptions of the interactions are not very general anymore. For first-principle calculations it does not matter what the surrounding of the atoms looks like. However, for the determination of the parameters it is important that the first-principle calculation is done in a similar situation in which the potentials will be used.

As aforementioned, the total energy calculated within the second moment approximation to the tight binding scheme is given by the equation (2.12).

In this approach both  $V$  and  $\phi$  are parameterized pair potentials, depending only on the distance between the two atoms for which the pair potential is



calculated. The first term is the repulsive part. This is purely due to pair-wise interactions. The last part is the attractive part and it has a multi-body kind of character.

The two parameterized pair potentials are given by the following two formulae<sup>9</sup>.

$$V(r) = Ae^{-p\left(\frac{r}{R_0}-1\right)} \quad , where: \quad A = \frac{q}{p-q} \frac{E_c}{Z} \quad (2.13)$$

and

$$\phi(r) = \xi^2 e^{-2q\left(\frac{r}{R_0}-1\right)} \quad , where: \quad \xi = \frac{p}{p-q} \frac{E_c}{\sqrt{Z}} \quad (2.14)$$

Here  $R_0$  is the first neighbor distance in the metal, depending on the crystallographic structure of the material and the lattice parameter and it is taken from values in literature. The behavior of these potentials is determined by the value of the parameters:  $p$ ,  $q$ ,  $E_c$  and  $Z$ . The values of these parameters can be determined by using information from experimental observations of the material under investigation or by using information that is gathered from results of first-principle calculations on the system of interest. We have chosen to determine the values of the parameters from the results of first-principle calculations. This is done because at a later stage parameters have to be determined for the interactions across the interface. It is most convenient to use the same methodology for determining the parameters.

### *Short range interactions across the interface*

For the modeling of the interactions across the interface, only pair-wise interactions are used. This yields the following equation for the energy of the interactions across the interface.

$$E_{tot} = \sum_i \sum_{j \neq i} V(|\vec{r}_{ij}|) \quad (2.15)$$

Here is  $V$  a simple pair potential (not to be confused with the repulsive pair interactions in Eq. (2.12)). We have chosen to employ the Buckingham potential<sup>10</sup> for this.

$$V(r) = \alpha e^{\frac{r}{R_0}} - \frac{D}{r^6} \quad (2.16)$$

As aforementioned, the behavior of this potential is governed by the values of the parameters that are used, which in our case are obtained with the help of first-principle calculations. This is done because the amount of useful information from experimental observations is rather limited.

The potential that is used so far for the description of the interactions across the interface are rather short range. It means that only a limited number of atoms interact with a certain atom. This is because of the sharp decay of the potential at distances larger than a few times the nearest neighbor distance. For a correct description of the interactions across a metal/ceramic interface, it is necessary to include also the long-range interactions between the atoms. The long-range interactions will be presented in the next section.

### *Long range interactions across the interface*

For a metal-ceramic interface, there is an additional interaction across the interface that is not present along interfaces between two metals. This is the interaction between charges in the ceramic and image charges in the metal. In a system with a metal-ceramic interface, image charges are being produced in the metal. These image charges are formed in the metal due to the charges of the ions in the ceramic. The charges in the ceramic give rise to a potential field and this potential field has a long distance interaction character extending into the metal. The electron gas in the metal interacts with this potential field. The result of this is that some locations are more attractive for the electrons of the metal atoms than other locations. A positively charged ion in the ceramic near the

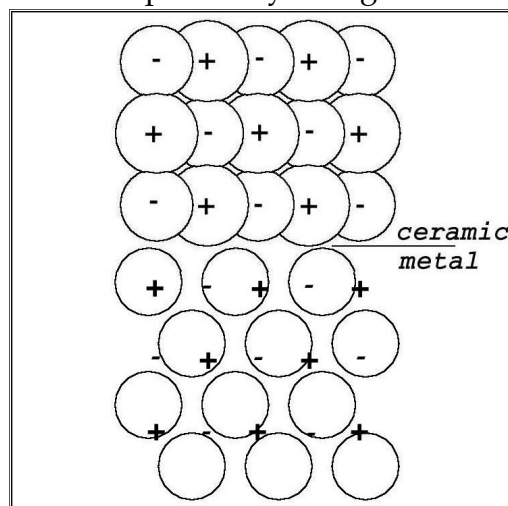


**Fig. 2-1:** Image charges formed in the metal under the influence of the ceramic ions.

interface results in a higher concentration of negative charges on the other side of the interface in the metal, and vice versa.

Thus the charges in the ceramic are mirrored in a virtual ‘mirror plane’, which runs parallel to the interface, somewhere between the metal and the ceramic. Positive charges in the ceramic tend to form an excessive concentration of electrons on the other side of the mirror plane, while negatively charged ions create depleted regions in the electron sea. This is schematically shown in Fig. 2-1.

The charges that are formed in the metal have the strongest interaction with the ions at the opposite side in the ceramic. These ions have charges with opposite sign. A negative charge concentration in the metal has the strongest interaction with the positive ion, which is located on the other side of the interface in the ceramic, and vice versa. The energy that is associated with the Coulomb interaction of two charges is given by the equation:

$$E_{ij} = \frac{1}{4\pi\epsilon} \frac{q_i q_j}{r_{ij}} \quad (2.17)$$

where  $q_i$  and  $q_j$  represent the charges of  $i$  respectively  $j$ , and  $r_{ij}$  is the distance between the two charges.

From Eq. (2.17), it can be seen that two charges with the same sign give a positive energy, whereas two charges with opposite signs give a negative contribution. It is concluded that image charges have the strongest interaction with oppositely charged ions in the ceramic and therefore energy is released upon forming the image charges. They cause an attractive force between the ceramic and the metal.

It can be concluded that to attain a description of the interaction between the metal and the ceramic that is physically sound, it is important to include the interactions between the charges in the ceramic and the image charges in the metal.

### *Discrete Classical Model*

One way to describe the image charges in the metal is by using charge densities and by performing a self-consistent calculation. This approach would lead us back to first-principle or similar calculations, which as we said before are too

complicated and computational too cumbersome to be realistic. Possibly in the future first-principle calculations will become feasible for these complicated systems. Therefore, we have to concentrate on a more simplified model that still gives a physical reasonable and adequate picture.

In the past, various models have been designed to describe the image charges. The three most important models are: the shell model<sup>11</sup>, the classical continuum model<sup>12</sup> and the discrete classical model<sup>13</sup>. In the shell model, it is assumed that the atoms have a shell, with a certain charge that is connected to the core with a spring. The shell is displaced with respect to the core in response to an electric field. The charge of the shell and the spring constant of the spring don't have a physical background and have to be fitted to first-principle calculations or to experimental observations.

Calculations<sup>14</sup> have been performed on aluminum faces in the presence of an electron above the surface. The calculations have been carried out using a first-principle approach, a classical continuum model and a discrete classical model. It is shown that the classical continuum model breaks down at smaller distances between the surface and the electron, while the discrete classical model is able to describe this situation rather well. This has been observed also for calculations with various orientations of the aluminum surface. The different orientations influence the results of the first-principle calculations and the results found with the discrete classical model, whereas the classical continuum model does not distinguish the different crystallographic orientations<sup>15</sup>.

The breakdown of the classical continuum model at smaller distances can be solved by limiting the fluctuations of the induced image charges that have wavelengths smaller than the Fermi wavelength. It has been shown<sup>16,17</sup> that the classical continuum model works well with this constraint. Despite this improvement, we have chosen to use the discrete classical model (DCM) because of the dependence on the surface orientation, which can be expected to influence the results of the calculations, but which is neglected in the classical continuum model.

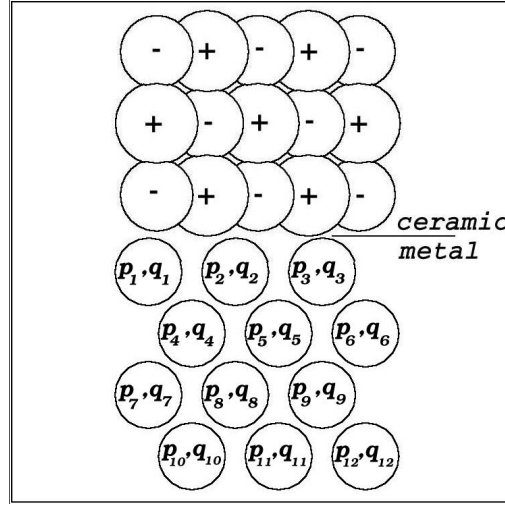


**Fig. 2-2:** Image charges and dipole moments, which are formed in the metal.

In the DCM, a description of the image charges is given by assuming that the image charges are restricted to the atomic sites in the metal. However, by doing this, problems arise with the physical interpretation of these interactions because the image charges are now limited to the atomic sites, instead of being able to be formed anywhere in the metal. To correct for this, dipole moments are introduced. The dipole moments are, like the calculated image charges, restricted to the atomic sites in the metal and are also formed under the influence of the potential generated by the ions in the ceramic. This is depicted in Fig. 2-2.

The potential in which the atoms are placed causes the atoms to become charged. This potential is the sum of the potentials of all the individual charges, image charges and dipole moments of the surrounding atoms. The potential at atomic site  $i$ , caused by a charge  $q_j$  at atomic site  $j$ , is given by:

$$\Phi_{q,ij} = \frac{1}{4\pi\epsilon} \frac{q_j}{|\vec{r}_{ij}|} \quad (2.18)$$

Here is  $\vec{r}_{ij}$  is the vector that gives the distance and the direction between the atomic sites. If a dipole moment with a strength  $\vec{p}_j$ , is located at the same atomic site instead of the charge then the potential caused by this dipole moment experienced at atomic site  $i$  is described by:

$$\Phi_{p,ij} = \frac{1}{4\pi\epsilon} \frac{\vec{p}_j \cdot \vec{r}_{ij}}{|\vec{r}_{ij}|^3} \quad (2.19)$$

The charge is assumed to be conserved at all times. The total charge of the metal including the image charges should be the same as the total charge of the metal without the image charges. To achieve this the potential at each atomic site is corrected with the average potential of all atomic sites.

This leads to the following description of the dependency of the image charge, formed at atomic site  $i$  ( $q_i$ ), on the potentials, which are described in the text above:

$$q_i = C \left( \Phi_0 - \sum_{j \neq i} (\Phi_{q,ij} + \Phi_{p,ij}) \right) \quad (2.20)$$

The relation between the image charge formed and the experienced potential is determined by the constant  $C$ . This constant is an indication how easy an atom is charged in response to a potential.  $C$  depends on the kind of metal that is placed in the potential.  $\Phi_0$  is included to ensure that the total charge of the metal stays equal to zero. It is equal to the average potential that is experienced on all the atomic sites.

The dipole moment that is formed on the atomic site is the result of the total electric field in which the atom is placed. The relation between the electric field and the potential is quite simple and it is described as:

$$\vec{E} = -\vec{\nabla}\Phi \quad \text{where: } \vec{\nabla} = \frac{\delta}{\delta x} \hat{x} + \frac{\delta}{\delta y} \hat{y} + \frac{\delta}{\delta z} \hat{z} \quad (2.21)$$

Combining Eq. 2.21 with Eq. 2.18 the potential generated by a charge results in:

$$\vec{E}_{q,ij} = \frac{1}{4\pi\epsilon} \frac{q_j}{|\vec{r}_{ij}|^3} \vec{r}_{ij} \quad (2.22)$$

For the dipole moment a similar combination is followed, and this yields the following:

$$\vec{E}_{p,ij} = \frac{1}{4\pi\epsilon} \frac{3(\vec{p}_j \cdot \vec{r}_{ij})\vec{r}_{ij} - |\vec{r}_{ij}|^2 \vec{p}_j}{|\vec{r}_{ij}|^5} \quad (2.23)$$

The dipole moment formed at an atomic site is equal to the total electric field, experienced at the atomic site multiplied by a constant ( $\alpha$ ). With this constant, a linear relation is made between the electric field in which the atom is placed

and the dipole moment that is formed. The value of this constant depends on the metal that is placed in the electric field:

$$\vec{p}_i = \alpha \left( \sum_{j \neq i} \vec{E}_{q,ij} + \vec{E}_{p,ij} \right) \quad (2.24)$$

As mentioned before, both the image charge and the dipole moment formed depend on a constant that is determined by the kind of metal that is placed on the atomic site. To calculate a value for these constants we assume that the atoms are perfect conducting spheres. To calculate the values for a perfectly conducting sphere it is necessary to know the radius of the sphere. We assume that the volume of the conducting sphere is equal to the volume occupied by an atom. The radius of such a sphere is called the Wigner-Seitz radius ( $R_{ws}$ ). With these assumptions, it is possible to calculate the value of the constant with:

$$C = 4\pi\epsilon R_{ws} \quad (2.25)$$

This gives the constant for the calculation of the image charge. For the constant of the dipole moment follows:

$$\alpha = 4\pi\epsilon R_{ws}^3 \quad (2.26)$$

Now we have all the necessary equations to calculate the image charges and the dipole moments on the atomic sites in the metal because of the potential and the electric field of the ions in the ceramic. In order to perform structure relaxations it is necessary to have the energy and the forces that are associated to these image charges and dipole moments.

Because the force can be easily deduced from the energy, i.e. by taking the gradient and adding a minus sign, we start with the equation for the energy. First, the energy of a charge in a potential is given by:

$$E_{q,i} = q_i \Phi_i = C(\Phi_0 - \Phi_i)\Phi_i \quad (2.27)$$

In addition, for the energy of a dipole moment in an electric field the following equation holds:

$$E_{p,i} = -\vec{p}_i \cdot \vec{E}_i = -\alpha |\vec{E}_i|^2 \quad (2.28)$$

In both equations, the second equality is the result of the previously presented equations for the size of the image charge in a potential and the size of a dipole moment in an electric field. From Eq. (2.28) is easy to see that the energy

associated with a dipole moment in the electric field results in a negative contribution. However, the energy associated with the image charge formed in a potential is not by definition negative. Nevertheless, it can be easily verified with some mathematical operations that the total energy associated with all the image charges is negative. This confirms what we stated before, namely: that the interaction between the image charges and the dipole moment in the metal with the charges in the ceramic should result in a negative contribution to the energy, and thus an attractive force between the metal and the ceramic.

Next, the individual forces that make up the total attractive force between the metal and the ceramic are derived. The force on an image charge in an electric field is given by:

$$\vec{F}_{q,i} = -\Delta E_{q,i} = 2q_i \vec{E}_i - \Phi_0 V \vec{E}_i \quad (2.29)$$

In addition, the force on a dipole moment is given by:

$$\vec{F}_{p,i} = -\Delta E_{p,i} = -2 \begin{pmatrix} p_{x,i} \frac{\delta^2}{\delta x^2} \Phi_i + p_{y,i} \frac{\delta^2}{\delta x \delta y} \Phi_i + p_{z,i} \frac{\delta^2}{\delta x \delta z} \Phi_i \\ p_{x,i} \frac{\delta^2}{\delta y \delta x} \Phi_i + p_{y,i} \frac{\delta^2}{\delta y^2} \Phi_i + p_{z,i} \frac{\delta^2}{\delta y \delta z} \Phi_i \\ p_{x,i} \frac{\delta^2}{\delta z \delta x} \Phi_i + p_{y,i} \frac{\delta^2}{\delta z \delta y} \Phi_i + p_{z,i} \frac{\delta^2}{\delta z^2} \Phi_i \end{pmatrix} \quad (2.30)$$

### *Fast Multipole Method*

For modeling of the metal-ceramic interface system, it is assumed that the computational cell is periodic in two directions parallel to the interface. In Fig. 2-3, a periodic potential is shown in one dimension for three computational cells and the potential in each computational cell should be repeated in the same way. In principle, it would be better to do simulations on an interface that is infinitely large and atomically flat (see Chapter 1), thereby eliminating the effects of the borders. However, this would mean that an infinite number of interactions among atoms have to be calculated and obviously, the calculation would never be finished! To limit the number of interactions between atoms a cut-off radius is introduced. Interactions for which the distance between the atoms is larger than the cut-off radius are assumed to have a negligibly small interaction and are not taken into account.



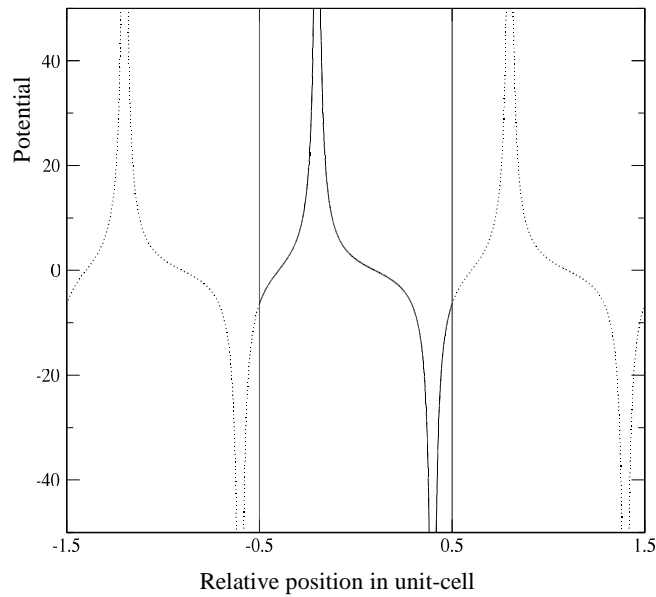


**Fig. 2-3:** The potential generated by 2 charges in each computational cell, the center cell and two neighboring cells are drawn.

The interactions between the charges in the ceramic and the image charges in the metal have a long-range character. The interaction between two charges has a much longer distance over which it can interact than the interaction between a charge and a dipole moment or the interactions between a dipole moment and another dipole moment. That the interaction between two charges is more long-ranged than the other interactions can be seen in the equations of the previous section. The Coulomb interaction between two charges shows an  $r^{-1}$  character, while the other interactions are either  $r^{-3}$  or  $r^{-5}$ , which are negligibly small at larger distances where the direct charge interaction is still significant large. Therefore, we further concentrate on the Coulomb interaction between two charges, because these interactions have the longest interaction distance and therefore generate most of the computational problems.

The long-range character means that the potential at a certain atomic site is influenced by the potential of a charge that is quite far away. If the cut-off radius for these interactions is taken too small, this results in image charges that can differ significantly from the image charges that are calculated with larger cut-off radii.

The cut-off radius for the Coulomb charge interactions should be several orders of magnitude larger than the cut-off radius that is used for the short-range interactions between the atoms. For the short-range interactions, it is possible to use one or two computational cells in each direction parallel to the interface in order to prevent problems with the periodic boundaries. The number of necessary computational cells depends on the size, along the directions parallel to the interface, of them with respect to the cut-off radius of the interactions.

Because the cut-off radius of the charge interactions is several orders of magnitude larger than the cut-off radius of the short-range interactions, it is virtually impossible to calculate the potential using Eq. (2.17) and (2.18). Therefore, to be able to calculate the charge interactions accurately and within a limited time we will use the so-called Fast Multipole Method (FMM)<sup>18, 19</sup>. The idea is to mimic the behavior of the charges, which are far away, with a smooth multipole expansion, while the charges at shorter distances are calculated in the normal way (see Eq. (2.18)), which requires more computational effort but is more accurate. In Fig. 2-4, an example is shown for a one-dimensional case. In

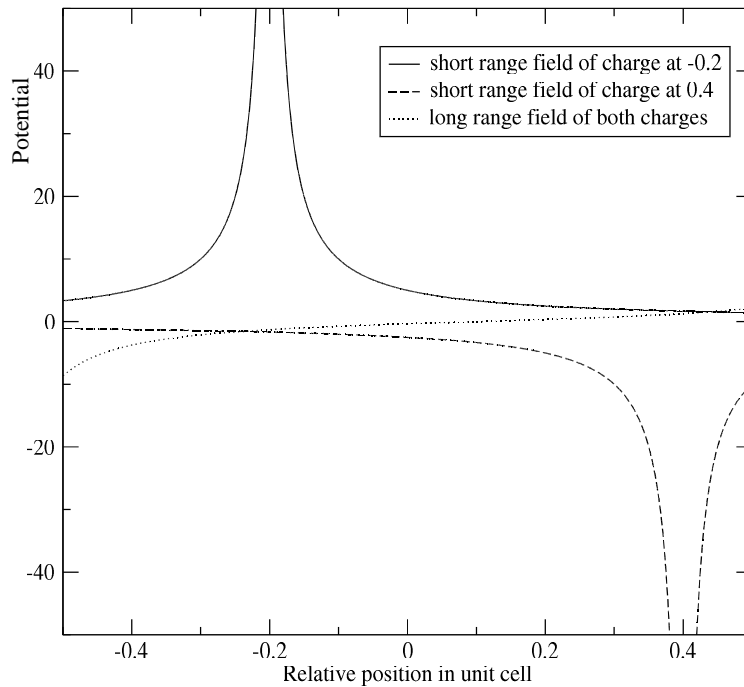


**Fig. 2-4:** Potentials arising from the 2 charges in the computational cell (at  $-0.2$  and  $0.4$ ), and from all the charges outside the computational cell.

this case, two charges are present in each computational cell, a positive to the left of the center and a negative to the right of the center. Three potential curves are drawn in the graph. They indicate the potentials in each position of the computational cell due to the charges in the same computational cell (2 lines) and due to the charges in the other computational cells. The solid line is of the positive charge left of the center of the computational cell, the dashed line is of the negative charge right of the center and the dotted line is for all the charges outside the computational cell. In the Fast Multipole Method, the last line is described with the help of a kind of Taylor expansion. This saves time of calculating the influence of all the other charges.

With this methodology, it is possible to calculate the potential that a certain atom experienced because of all the charges that are farther away than a couple computational cells. The potentials that are closer to the atom cannot be described with this method because at shorter distances the interaction fluctuates heavily. Indeed, these larger fluctuations would require a better expansion by including more terms in the series expansion. Of course, this requires a larger computational effort. Therefore, a choice has to be made which part of the interactions has to be calculated with multipoles and which part directly. Fig. 2-4 displays the potential due to different charges, i.e. the charges in the same computational cell and the charges outside the computational cell. In Fig. 2-5, the potential due to charges outside the computational cell is depicted on the left. To the right, the potential is shown due to the charges from

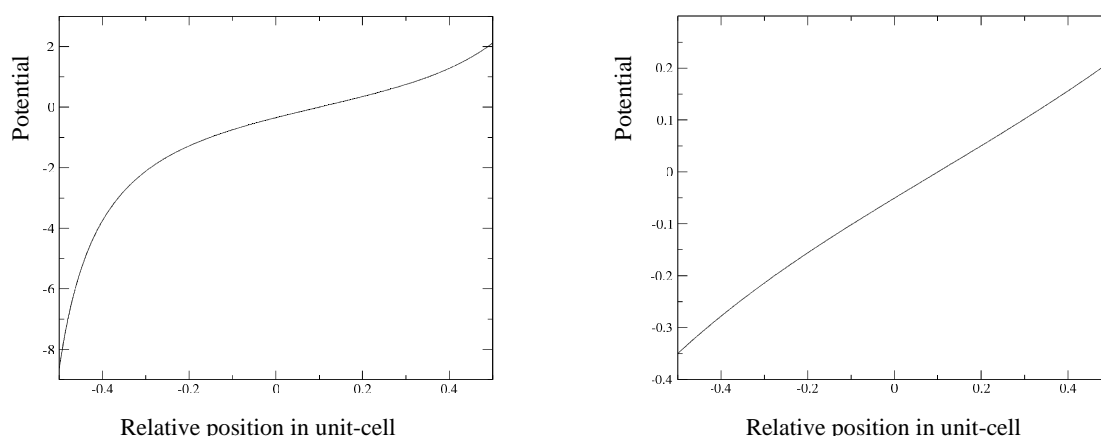


**Fig. 2-5:** Potential of charges far away, with two different minimal distances.

all the computational cells, excluding the central computational cell and the first neighboring computational cells. Besides the maximal absolute value of both graphs, which drops from 9 to 0.4, it should be noted that the graph on the right is rather straight compared with the left one. This indicates that the right graph is much easier to describe with an expansion than the left one.

Important equations for the Fast Multipole Expansion are summarized as follows: The first equation gives the potential in point  $P$ , due to  $k$  charges. The spherical coordinates of point  $P$  are  $(r, \theta, \phi)$  and of the charges  $(\rho_i, \alpha_i, \beta_i)$ , the sizes of the charges are  $q_i$ . A condition is that all the charges are closer to the origin than point  $P$ .

$$\Phi(P) = \sum_{n=0}^{\infty} \sum_{m=-n}^n \frac{M_n^m}{r^{n+1}} Y_n^m(\theta, \phi) \quad (2.31)$$

where

$$M_n^m = \sum_{i=1}^k q_i \rho_i^n Y_n^{-m}(\alpha_i, \beta_i) \quad (2.32)$$

In Eq. (2.31) and (2.32) spherical harmonics are used. They can be expressed as function of the associated harmonics with the following equation

$$Y_n^m(\theta, \phi) = \sqrt{\frac{(n-|m|)!}{(n+|m|)!}} P_n^{|m|}(\cos \theta) e^{im\phi} \quad (2.33)$$

In Eq. (2.31) and (2.32) it can be seen that only the expansion constants  $M_n^m$  depend on the size of the charges and the coordinates of the charges. The result of this is that once the constants are known the time required for the calculation of the potential does not depend on the number of charges.

With the Eq. (2.31) it is possible to calculate the expansion of all the charges in one computational cell. For further calculations, it is necessary to transfer the expansions from a certain point to another point. This can be done as follows.

$$\Phi(P) = \sum_{n=0}^{\infty} \sum_{m=-n}^n \frac{O_n^m}{r'^{n+1}} Y_n^m(\theta', \phi') \quad (2.34)$$

First the expansion of charges around point  $Q=(\rho, \alpha, \beta)$  is given for point  $P=(r, \theta, \phi)$ , and  $P-Q=(r', \theta', \phi')$ .

## CHAPTER 2

Note that this expansion is centered on point Q, but this can be converted to an expansion around the origin with the following equation:

$$\Phi(P) = \sum_{j=0}^{\infty} \sum_{k=-j}^j \frac{M_j^k}{r^{j+1}} Y_j^k(\theta, \phi) \quad (2.35)$$

where

$$M_j^k = \sum_{n=0}^j \sum_{m=-n}^n \frac{O_{j-n}^{k-m} \cdot J_m^{k-m} \cdot A_n^m \cdot A_{j-n}^{k-m} \cdot \rho^n \cdot Y_n^{-m}(\alpha, \beta)}{A_j^k} \quad (2.36)$$

The values of  $A_n^m$  and  $J_n^m$  are given by:

$$A_n^m = \frac{(-1)^n}{\sqrt{(n-m)!(n+m)!}} \quad (2.37)$$

and

$$J_n^m = \begin{cases} (-1)^{\min(|m|, |n|)} & \text{if } m \cdot n < 0 \\ 1 & \text{otherwise} \end{cases} \quad (2.38)$$

Now we are able to determine the multipole expansion of the charges in one computational cell and translate this multipole expansion in such a way that we also have the expansion of other computational cells.

We are interested in one expansion that describes the potential due to the charges outside the computational cell. To achieve this the multipole expansions are transformed to local expansions. Again the charges are in a sphere around  $Q=(\rho, \alpha, \beta)$ , but now the potential is calculated for  $P=(r, \theta, \phi)$ , which is located in a sphere around the origin.

$$\Phi(P) = \sum_{j=0}^{\infty} \sum_{k=-j}^j L_j^k \cdot Y_j^k(\theta, \phi) \cdot r^j \quad (2.39)$$

where

$$L_j^k = \sum_{n=0}^{\infty} \sum_{m=-n}^n \frac{O_n^m \cdot J_m^m \cdot A_n^m \cdot A_j^k \cdot Y_{j+n}^{m-k}(\alpha, \beta)}{A_{j+n}^{m-k} \cdot \rho^{j+n+1}} \quad (2.40)$$

Again, the value of  $A_n^m$  is given by Eq. (2.37) and the value of  $J_n^m$  is given by:

$$J_n^m = \begin{cases} (-1)^m (-1)^{\min(|m|, |n|)} & \text{if } m \cdot n > 0 \\ (-1)^m & \text{otherwise} \end{cases} \quad (2.41)$$

The final step is to convert to the local expansion. The origin of the local expansion is located at  $Q=(\rho, \alpha, \beta)$  and the potential are calculated in  $P=(r, \theta, \phi)$  and  $P-Q=(r', \theta', \phi')$ . The potential calculated with the original local expansion is given by (2.42).

$$\Phi(P) = \sum_{n=0}^{\infty} \sum_{m=-n}^n O_n^m \cdot Y_n^m(\theta', \phi') \cdot r'^n \quad (2.42)$$

The potential calculated with the translated expansion is given by

$$\Phi(P) = \sum_{j=0}^{\infty} \sum_{k=-j}^j L_j^k \cdot Y_j^k(\theta, \phi) \cdot r^j \quad (2.43)$$

where

$$L_j^k = \sum_{n=j}^{\infty} \sum_{m=-n}^n \frac{O_n^m \cdot J_{n-j, m-k}^m \cdot A_{n-j}^{m-k} \cdot A_j^k \cdot Y_{n-j}^{m-k}(\alpha, \beta) \cdot \rho^{n-j}}{A_n^m} \quad (2.44)$$

The value of  $A_n^m$  is again given by Eq. (2.37) and the value of  $J_{n,m}^{m'}$  is given by:

$$J_{n,m}^{m'} = \begin{cases} (-1)^n (-1)^m & \text{if } m \cdot m' < 0 \\ (-1)^n (-1)^{m'-m} & \text{if } m \cdot m' > 0 \text{ and } |m'| < |m| \\ (-1)^n & \text{otherwise} \end{cases} \quad (2.45)$$

With these equations, it is possible to calculate the potential for points inside the computational cell due to charges in other computational cells. For further proves of the various steps reference is made to literature.

## 2.4 Final requirements for structural relaxations

The necessary models for the description of the interactions between the atoms near a metal/ceramic interface are now explained. However, before structural relaxations can be performed a few open questions still remain. What are the actual values of the parameters of the pair potentials, and how are the calculated forces used in the relaxation procedure?

First-principle calculations are performed on rather simplified models; these calculations are performed by making use of the basic modules in the Castep program. The computational cells that are used in the first-principle calculations contain at most a couple of dozen atoms. The calculations are performed on multiple computational cells. In these calculations the distance

between the metal and the ceramic, the positioning of the metal parallel to the interface with respect to the ceramic and/or the lattice parameters of the computational cell can be varied. In the first-principle calculations, a wide range of interface distances is governed.

From the results of the first-principle calculations, the energies are extracted as well as the forces on the metal atoms. This information is also calculated with potentials for which the parameters have to be determined. From the results of the first-principle calculations and of the potentials, the deviation can be calculated indicating whether the first-principle calculations are represented well by parameterized potentials. This deviation is used to optimize the values of the parameters of the potentials in such a way that the results of the potentials come as close as possible to the results of the first-principle calculations.

During the structure relaxations, which are performed by using a computer code written in our group, the forces are calculated on the metal atoms that result from the interactions within the metal, the short-range interactions across the interface and the long-range interactions across the interface. The atoms are displaced in the direction where the gradient of the energy is the largest. This is done in such a way that no oscillation occurs and that the displacements in each step are as large as possible. This procedure can be used because we are only interested in the final configuration of the atoms and not in the dynamic behavior of the atoms.

In the calculations, the ions in the ceramic have a fixed position and the atoms of the metal far away from the interface are also fixed. The former choice is made because the metal is softer than the ceramic. Therefore, the largest portion of the relaxations will take place in the metal and not in the ceramic. The second choice is made to prevent the influence of free surfaces. This results in a system in which the metal atoms are in a fixed space, which does not necessarily result in a stress free solution perpendicular to the interface.

To overcome the problem of the possible stress perpendicular to the interface, a solution is chosen in which the energy of the system is calculated for different interface separations. The interface separation with the lowest energy is used as the interface separation in the next relaxation step of the metal atoms. This step is performed at regular intervals.

After the relaxations are finished, the work of adhesion is calculated for the system under investigation. The work of adhesion is calculated by subtracting the total energy of the relaxed interface system in which the interface separation infinite is from the total energy of the relaxed interface system with the optimal interface separation (see for a discussion, Chapter 1).

## 2.5 Conclusion

A model is presented that is used to perform structure relaxations on metal/ceramic interface systems. The model is designed in such a way that the interactions are derived from a physical description being tractable from a computational viewpoint. The accuracy of the model will be illustrated in the next chapters in which the results for various interface systems are presented.

## 2.6 References

- 1 S.Gasiorowicz, *Quantum mechanics*, John Wiley & Sons, Inc., 1974
- 2 A.P.Sutton and R.W.Baluffi, *Interfaces in Crystalline Materials*, Clarendon Press, 1995
- 3 P.Hohenberg and W.Kohn, *Phys.Rev.B*, **136**, B864 (1964)
- 4 W.Kohn and L.J.Sham, *Phys.Rev.A*, **140**, 1133 (1965)
- 5 J.Harris, *Phys.Rev.B*, **31**, 1770 (1985)
- 6 W.M.C.Foulkes and R.Haydock, *Phys.Rev.B*, **39**, 12520 (1989)
- 7 A.P.Sutton, P.D.Godwin and A.P.Horsfield, *MRS-Bulletin*, **21**, 42 (1996)
- 8 S.M.Foiles, *MRS-Bulletin*, **21**, 24 (1996)
- 9 V.Rosato, M.Guillope and B.Legrand, *Phil.Mag.A*, **59**, 321 (1989)
- 10 D.M.Duffy, J.H.Harding and A.M.Stoneham, *Acta Mater.*, **44**, 8 (1996)
- 11 M.Stoneham, J.Harding and T.Harker, *MRS-Bulletin*, **21**, 29 (1996)
- 12 D.M.Duffy, J.H.Harding and A.M.Stoneham, *Acta metal. Mater.*, **40**, S11 (1992)
- 13 M.W.Finnis, *Acta metal. Mater.*, **40**, S25 (1992)
- 14 M.W.Finnis, *Surface Science*, **241**, 61 (1991)
- 15 M.W.Finnis, R.Kaschner, C.Kruse, J.Furthmüller and M.Scheffler, *J.Phys.: Condens. Matter*, **7**, 2001 (1995)
- 16 J.Purton, S.C.Parker and D.W.Bullet, *J.Phys.: Condens. Matter*, **9**, 5709 (1997)



## CHAPTER 2

- 17 D.M.Duffy, J.H.Harding and A.M.Stoneham, *Phil.Mag.A*, **67**, 865 (1993)
- 18 L.F.Greengard, *The rapid evaluation of potential fields in particle systems*, MIT Press, 1987
- 19 L.Greengard and V.Rokhlin, *Journal of Computational Physics*, **73**, 325 (1987)